

THE ACTIVE PNEUMATIC-BALANCED CONTROLLED LIFTING POSITIONING SYSTEM FOR THE NEW GENERATION TFT-LCD GLASS SUBSTRATES

Mao-Hsiung CHIANG^{*}, Yih-Nan CHEN^{*,**}, Fei-Lung YANG^{****}, Wei-Chieh CHEN^{***} and
Hong-Chuen HSIEH^{***}

^{*} Department of Engineering Science and Ocean Engineering,
National Taiwan University
Taipei 106, Taiwan
(E-mail: mhchiang@ntu.edu.tw)

^{**} Department of Mechanical Engineering,
Tatung University
Taipei 104, Taiwan

^{***} Graduate Institute of Automation and Control,
National Taiwan University of Science and Technology,
Taipei 106, Taiwan

^{****} Department of Mechanical Engineering,
Nanya Institute of Technology,
Taoyuan 320, Taiwan

ABSTRACT

Due to the development of the larger size of FPD, the conveyor system, especially the lifting system, become a significant topic. This paper aims to develop novel lifting system with the AC servo driving and the pneumatic-balanced system for the new generation of LCD glass substrates. Owing to the large variation range of the loading in the new generation lifting system, the pneumatic-balanced system is developed for counterbalanced the weight of the loading for reducing the loading power of the AC servo motor. A PC-Based control system is developed for achieving better response and position accuracy. Adaptive sliding mode control with function approaching technique is used in this paper as the control strategy. In order to improve the jerk problem during the motion process, path control is used. The proposed new lifting system with pneumatic-balanced technique is implemented and verified through simulation and experiment.

KEY WORDS

Pneumatic-balanced control, Path-positioning control, Lifting system, Glass substrate, Flat panel display.

INTRODUCTION

Flat Panel displays (FPD) have become one of the most significant industries in the world. The manufacturers of FPD concentrate especially on the countries in east-Asia, including Taiwan, Japan and Korea. In order to satisfy the fast development of the request of the market that trends toward larger and larger sizes for TV and monitor,

the new generations of the glass substrates have been developed almost every three years. However, the weights and the dimensions of the glass substrates also increase such that the manufacturing equipments have to face new process challenge. Table 1 shows the dimension and weight of the different generation of glass substrates. The thickness of the glass substrate is about 0.5 to 0.7 mm.

Table 1 Dimension of different generation of glass substrate

Generation	Size (mm ²)	Weight (kgf)
2nd Gen	400×500	0.4
3rd Gen	550×670	0.7
3.5th Gen	600×720	0.8
4th Gen	680×880	1.1
5th Gen	1100×1250	2.5
5.5th Gen	1300×1500	3.5
6th Gen	1500×1850	5
7th Gen	1800×2000	6.5
7.5th Gen	1950×2250	7.5
8th Gen	2160×2460	9.0

The conveyor systems of the glass substrate become more and more complex due to the increase of the dimension and weight of the glass substrate. The conveyor systems of the glass substrate contain horizontal linear conveyor, horizontal rotational conveyor and vertical lifting system. The horizontal linear conveyors are driven by roller generally and can be supported by air bearing in the new generation. The horizontal rotational conveyor rotates the glass substrates. The vertical lifting systems serve to load the glass substrate in and out the cassette, which works as buffer of glass substrate in the process. This paper aims to investigate the lifting positioning system with pneumatic-balanced system. In the new generation of glass substrates, the weight variation between no-load and full-load conditions of the lifting system can reach from 200 kgf to 1000 kgf. The large loading variation results in the demand of larger power of the AC servo motor for positioning. Instead of that, the loading variation can be counter-balanced by the pneumatic cylinders of the pneumatic-balanced system such that the AC servo motor needs only smaller power without adding the inertial mass. Besides, in order to achieve jerk-free motion, path-positioning control, that contains path tracking control in the motion process and positioning control at the target end position, is developed in this paper. For that, adaptive sliding mode control is used to develop the controller.

TESTRIG LAYOUT

The test rig of the active pneumatic-balanced lifting positioning system for the new generation TFT-LCD glass substrate consists of the pneumatic-balanced controlled system, which contains two rodless pneumatic cylinders with pressure control servo valves, and a positioning control system driven by an AC servo

motor with belt transmission mechanism that serves as position control of the lifting system. The pneumatic-balanced controlled system serves to balance actively the weight of the loading and the lifting table.



Figure 1 Layout of the test rig

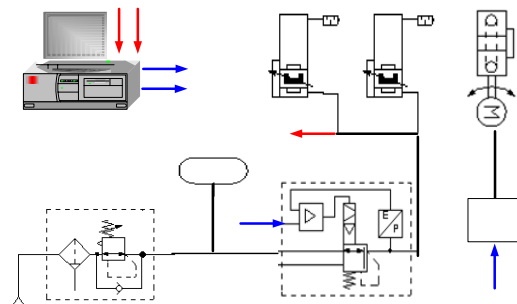


Figure 2 Concept of the test rig

Table 2 Specifications of the test rig

Item	Specifications
Control type	Path-positioning
Glass substrate dimension	1950 X 2250mm
Weight of full loading	1000kg
Weight of no-loading	200kgf
Stroke of Z-axis	1100mm
Velocity	40m/min
Class of clean room	5000
Position accuracy of Z-axis	+/-0.2mm

A PC-based control system is used to implement the positioning control and the pneumatic-balanced control. Figure 1 photographically shows the layout of the test rig. Figure 2 schematically illustrates the concept of the proposed pneumatic-balanced lifting positioning system. The pneumatic balanced control system works firstly to keep the resultant weight constant, which means the weight of loading minus the counter-balanced force form the pneumatic cylinders is constant. Pressure sensors are used to measure the pneumatic pressure p and calculate the pneumatic balanced force F_{pneu} by

$$F_{pneu} = p \cdot A \cdot n \quad (1)$$

where A indicates the effective piston area of pneumatic cylinder; n is the cylinder number. The positioning control system driven by an AC servo motor is measured by a position sensor. Table 2 specifies the required performance.

ADAPTIVE FUZZY SLIDING MODE CONTROL

Designing a SMC needs to know the system models and to find the inverse form of inertia term in system dynamics. However, the accurate mathematical models are always difficult to formulate or even not available. To solve these problems, an AFSMC shown in Fig.3 is proposed.

The state equations of the servo control system model can be achieved as follows

$$\begin{aligned} \dot{x}_1 &= x_2(t) \\ \dot{x}_2 &= -\sum_1^2 a_i x_i(t) + g(x)u + d(x) = f(x) + g(x)u + d(x) \end{aligned} \quad (2)$$

Fuzzy Control

Assume that there are n rules in a fuzzy base and each of them has the following form:

$$R^i : \text{IF } S \text{ is } F^i \text{ THEN } u \text{ is } \alpha_i \quad (3)$$

where S is the input variable of the fuzzy system; u is the output variable of the fuzzy system; F^i are the triangular-type membership functions; and α_i are the singleton control actions for $i = 1, 2, \dots, n$. The defuzzification of the FC output is accomplished by the method of center-of-gravity (Lee 1990)

$$u = \sum_{i=1}^n \alpha_i \times w_i / \sum_{i=1}^n w_i = \underline{\alpha}^T \underline{\xi} \quad (4)$$

where w_i is the firing weight of the i th rule, $\underline{\alpha} = [\alpha_1, \alpha_2, \dots, \alpha_n]^T$ is the parameter vector and $\underline{\xi} = [\xi_1, \xi_2, \dots, \xi_n]^T$ is the vector of fuzzy basis functions

$$\xi_i = w_i / \sum_{i=1}^n w_i \quad (5)$$

For the conventional FC, the control actions α_i should be previously assigned through a lot of trails to achieve satisfactory control performance. In the following, the adaptive algorithm will be proposed to tune these control actions on-line.

Fuzzy Sliding Mode Control

The methods to design the fuzzy sliding-mode controller for a non-linear system with 2nd order where the error and the error change rate were used to synthesize fuzzy reasoning rules was proposed (Palm 1994 and Hwang *et al.* 1992). However, the rule number was larger and did not give the mathematical expression. Thus, it is difficult to analyze the properties of the control system. To overcome this problem, we adopt the sliding surface $S = 0$ of SMC as a variable to compress all the information into one type, extend the sliding surface $S = 0$ to the fuzzy sliding surface $\tilde{S} = \tilde{0}$, and make S be a linguistic description of \tilde{S} . In this paper the two triangular-typed functions are used to define the membership functions of IF-part and THEN-part, which are depicted in Figs.4 (a) and 4(b) respectively. The fuzzy rules are given in the following form

$$R^l : \text{IF } S \text{ is } \tilde{F}_s^l \text{ THEN } u_{fs} \text{ is } \tilde{F}_u^{8-l}, l = 1, \dots, 7. \quad (6)$$

According to the sup-min compositional rule of inference and the defuzzification of the control output accomplished by the method of center-of-area, the mathematical expression can be derived as

$$u_{fs} = \begin{cases} 1 & , \text{if } z < -1 \\ (7.5z^2 + 13.5z + 5)/(9z^2 + 15z + 5) & , \text{if } -1 \leq z < -2/3 \\ (9z^2 + 11z + 2)/(18z^2 + 18z + 2) & , \text{if } -2/3 \leq z < -1/3 \\ (1.5z^2 + 1.5z)/(9z^2 + 3z - 1) & , \text{if } -1/3 \leq z < 0 \\ (-1.5z^2 + 1.5z)/(9z^2 - 3z - 1) & , \text{if } 0 \leq z < 1/3 \\ (-9z^2 + 11z - 2)/(18z^2 - 18z + 2) & , \text{if } 1/3 \leq z < 2/3 \\ (-7.5z^2 + 13.5z - 5)/(9z^2 - 15z + 5) & , \text{if } 2/3 \leq z < 1 \\ -1 & , \text{if } z \geq 1 \end{cases} \quad (7)$$

where $z = S/\Phi$ and $\Phi > 0$ is a constant which describes the width of a boundary layer. As $|S| \geq \Phi$, it is easy to check $u_{fs} = -\text{sgn}(S)$.

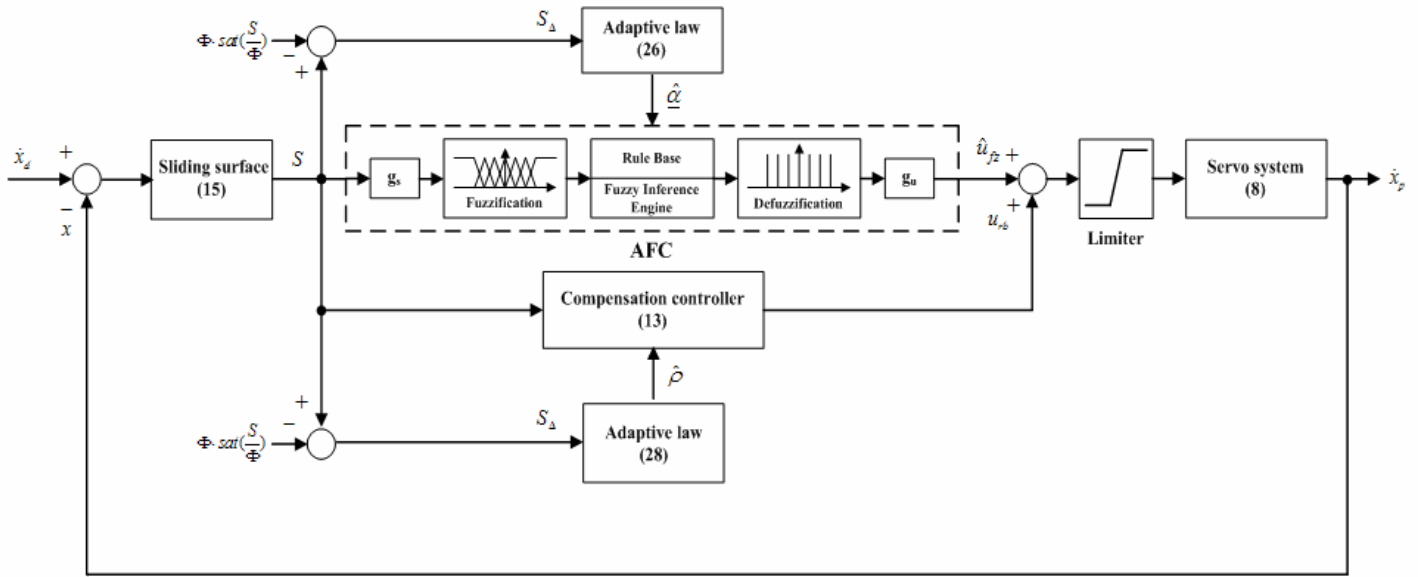


Figure 3 Adaptive fuzzy sliding mode control

Adaptive Fuzzy Sliding Mode Control System

The control objective is to find a control law so that the hydraulic actuator can track the desired velocity $\dot{x}_d(t)$.

Define the tracking error $e(t)$ as

$$e(t) = \dot{x}_d(t) - \dot{x}_p(t) \quad (8)$$

where $\dot{x}_p(t)$ is the control output and $\dot{x}_d(t)$ is the desired velocity. Then define a sliding surface as

$$S(t) = \dot{e}(t) + k_1 e(t) \quad (9)$$

where k_1 is non-zero positive constants. Assume that parameters of the system in (2) are well known and the external load disturbance is measurable, then we can take the control law as

$$u^* = g^{-1}(x)[\eta S_\Delta(t) - f(x) - d(x) + \ddot{x}_d + k_1 \dot{e}(t)] \quad (10)$$

where $S_\Delta(t) = S(t) - \Phi \text{sat}(S(t)/\Phi)$. The function S_Δ has several properties as below that are useful in the design of adaptive law (Sanner *et al.* 1992).

Property1: When $|S| > \Phi$, $|S_\Delta| = |S| - \Phi$ and $\dot{S}_\Delta = \dot{S}$.

Property2: When $|S| \leq \Phi$, $S_\Delta = \dot{S}_\Delta = 0$.

The above properties of the boundary layer concept are to be exploited, in the design of AFSMC, our goal being to cease adaptation as soon as the boundary layer is reached. This approach aims to avoid the possibility of unbounded growth. Differentiating (9) along the system trajectories (2), we have

$$\dot{S}(t) = -f(x) - g(x)u - d(x) + \ddot{x}_d + k_1 \dot{e}(t) \quad (11)$$

Substituting (10) into (11) gives

$$\dot{S}(t) + \eta S_\Delta(t) = 0, \quad \eta > 0. \quad (12)$$

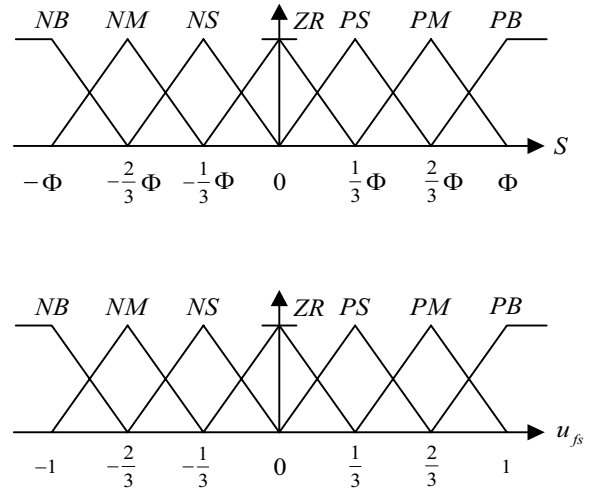


Figure 4 Fuzzy partitions and membership functions of S and u_{fs} in the respective universe of discourse

Equ. (12) shows that $e(t)$ will converge to the neighbour of zero as $t \rightarrow \infty$ and the value of the neighbourhood are relative to the value of Φ (Slotine *et al.* 1896). However, the system parameters may be unknown or perturbed; the controller u^* cannot be precisely implemented. Therefore, by the universal approximation theorem (Lee *et al.* 2001), an optimal fuzzy control $\hat{u}_{fz}(S, \underline{\alpha}^*)$ in the form of (4) exists such that the approximation error of fuzzy controller can be defined as

$$|u^* - \hat{u}_{fz}(S, \underline{\alpha}^*)| = \rho^* \quad (13)$$

where ρ^* is the inherent approximation error and is assumed to be bounded by $|\rho^*| \leq M$. Employing a fuzzy controller

$$\hat{u}_{fz}(S, \hat{\underline{\alpha}}) \text{ to approximate } u^* \text{ as}$$

$$\hat{u}_{fz}(S, \hat{\underline{\alpha}}) = \hat{\underline{\alpha}}^T \underline{\xi} \quad (14)$$

where $\hat{\underline{\alpha}}$ is the estimated values of $\underline{\alpha}^*$. The control law for the developed AFSMC is assumed to take the following form:

$$u = \hat{u}_{fz}(S, \hat{\underline{\alpha}}) + u_{rb}(S) \quad (15)$$

where the fuzzy controller \hat{u}_{fz} is designed to approximate the control u^* and the robust controller u_{rb} is designed to compensate the difference between the controller u^* and fuzzy controller $\hat{u}_{fz}(S, \hat{\underline{\alpha}})$. Through (10), (11) and (15) the dynamical equation as follow can be derived:

$$\dot{S}(t) + \eta S_{\Delta}(t) = g[u^* - \hat{u}_{fz}(S, \hat{\underline{\alpha}}) - u_{rb}(S)] \quad (16)$$

In order to derive the adaptive laws that ensure convergence to the boundary layer, a candidate Lyapunov function is defined as:

$$V(S_{\Delta}, \tilde{\underline{\alpha}}, \tilde{\rho}) = \frac{1}{2} \frac{S_{\Delta}^2}{g} + \frac{1}{2\eta_1} \tilde{\underline{\alpha}}^T \tilde{\underline{\alpha}} + \frac{1}{2\eta_2} \tilde{\rho}^2 \quad (17)$$

where $\tilde{\underline{\alpha}}^T = \underline{\alpha}^{*T} - \hat{\underline{\alpha}}^T$ and $\tilde{\rho} = \rho^* - \hat{\rho}$ are the approximation error of the parameter vectors $\underline{\alpha}^{*T}$ and ρ^* respectively. In addition, η_1 and η_2 are positive constants. Differentiate (17) with respect to time as

$$\dot{V}(S_{\Delta}, \tilde{\underline{\alpha}}, \tilde{\rho}) = S_{\Delta} \dot{S}_{\Delta} / g + \tilde{\underline{\alpha}}^T \dot{\tilde{\underline{\alpha}}} / \eta_1 + \tilde{\rho} \dot{\tilde{\rho}} / \eta_2. \quad (18)$$

Thus, if $|S| \leq \Phi$, then $S_{\Delta} = 0$, it follows $\dot{V}(S_{\Delta}, \tilde{\underline{\alpha}}, \tilde{\rho}) = 0$. If $|S| > \Phi$, then $\dot{S}_{\Delta} = \dot{S}$. By substituting (16) into (18), (19) can be obtained

$$\begin{aligned} \dot{V}(S_{\Delta}, \tilde{\underline{\alpha}}, \tilde{\rho}) &= -\eta S_{\Delta}^2 / g + S_{\Delta} [u^* - \hat{u}_{fz}(S, \hat{\underline{\alpha}})] - S_{\Delta} u_{rb}(S) + \tilde{\underline{\alpha}}^T \dot{\tilde{\underline{\alpha}}} / \eta_1 + \tilde{\rho} \dot{\tilde{\rho}} / \eta_2 \\ &= -\eta S_{\Delta}^2 / g + S_{\Delta} [u^* - \hat{u}_{fz}(S, \hat{\underline{\alpha}}) + \hat{u}_{fz}(S, \hat{\underline{\alpha}}) - u_{rb}(S)] - S_{\Delta} u_{rb}(S) + \tilde{\underline{\alpha}}^T \dot{\tilde{\underline{\alpha}}} / \eta_1 + \tilde{\rho} \dot{\tilde{\rho}} / \eta_2 \\ &\leq -\eta S_{\Delta}^2 / g + |S_{\Delta}| |u^* - \hat{u}_{fz}(S, \hat{\underline{\alpha}})| + S_{\Delta} [\hat{u}_{fz}(S, \hat{\underline{\alpha}}) - u_{rb}(S)] - S_{\Delta} u_{rb}(S) + \tilde{\underline{\alpha}}^T \dot{\tilde{\underline{\alpha}}} / \eta_1 + \tilde{\rho} \dot{\tilde{\rho}} / \eta_2 \\ &= -\eta S_{\Delta}^2 / g + |S_{\Delta}| \rho^* - S_{\Delta} u_{rb}(S) - \tilde{\rho} \dot{\tilde{\rho}} / \eta_2 + \tilde{\underline{\alpha}}^T (S_{\Delta} \underline{\xi}(S) - \dot{\hat{\underline{\alpha}}}) / \eta_1 \end{aligned} \quad (19)$$

For achieving $\dot{V}(S_{\Delta}, \tilde{\underline{\alpha}}, \tilde{\rho}) < 0$, the adaptive laws of AFSMC are chosen as

$$\dot{\hat{\underline{\alpha}}} = \eta_1 S_{\Delta} \underline{\xi}(S) \quad (20)$$

$$u_{rb}(S) = -\hat{\rho} u_{fs} \quad (21)$$

$$\dot{\hat{\rho}} = \eta_2 |S_{\Delta}| \quad (22)$$

Then (19) can be rewritten as

$$\dot{V}(S_{\Delta}, \tilde{\underline{\alpha}}, \tilde{\rho}) \leq -\eta S_{\Delta}^2 / g \quad (23)$$

Equations (20)-(23) only guarantee that $S_{\Delta} \in L_{\infty}$, but do not guarantee convergence. Integrating both sides of (23) and some derivations yields

$$\int_0^{\infty} S_{\Delta}^2 dt \leq \frac{V(S_{\Delta}(\infty), \tilde{\underline{\alpha}}, \tilde{\rho}) - \dot{V}(S_{\Delta}(0), \tilde{\underline{\alpha}}, \tilde{\rho})}{\eta/g} \quad (24)$$

Since the right side of (24) is bounded, $S_{\Delta} \in L_2$. Using Barbalat's lemma (Slotine *et al.* 1991) it can be shown that $\lim_{t \rightarrow \infty} S_{\Delta} = 0$. This means that inequality $|S| \leq \Phi$ is obtained asymptotically. Thus, the tracking error $e(t)$ converges to a neighbourhood of zero. In summary, the AFSMC system is shown in (15), where \hat{u}_{fz} is given in (20) with the parameters $\hat{\underline{\alpha}}$ adjusted by (20); u_{rb} is given in (21) with the parameter $\hat{\rho}$ adjusted by (22). By applying this estimation law, the AFSMC system can be guaranteed to be stable in the Lyapunov sense.

EXPERIMENTS

In order to verify the new pneumatic-balanced lifting positioning system with the proposed control strategy, experiments with variable motion under different conditions are implemented. Figure 5 shows the experimental results of the multi-step positioning control with 100mm of each stroke within 12 sec in no-loading conditions. The ramp path is given between the positioning points. The pneumatic-balanced pressure is 0.32MPa. Besides, the multi-step positioning control with 200mm of each stroke within 14 sec is also implemented and compared in Table 3.

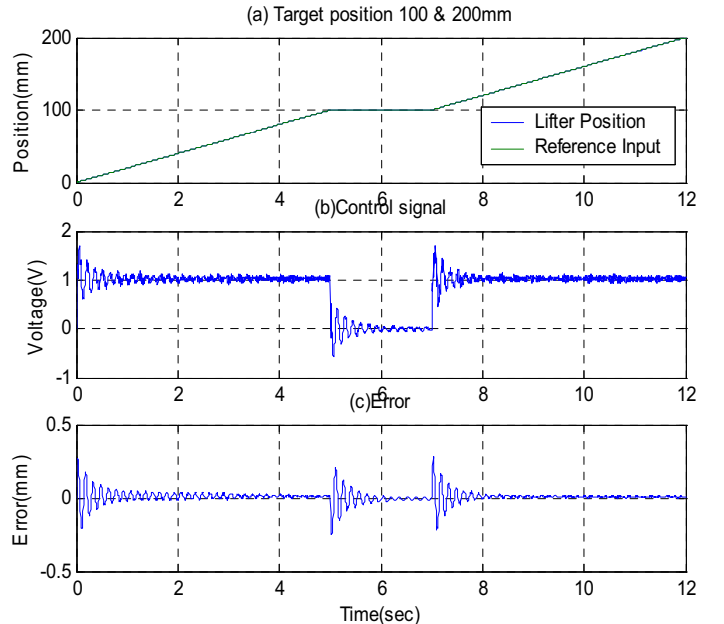


Figure 5 Experimental results of multi-step positioning control

Table 3 Positioning control performance comparison

Multi-step positioning control			
Stroke (mm)	duration (sec)	Max.tracking error(mm)	End point error(mm)
100	0-5	0.279	0.009
200	7-12	0.279	0.006

Figure 6 shows the experimental results of the path-positioning control with 500mm within 5 sec in no-loading conditions. A jerk-free path is given between the positioning points. The pneumatic-balanced pressure is 0.32MPa. Besides that, the path-positioning control experiments with 100 and 300mm within 5 and 10 sec are also implemented and compared in Table 4.

From the comparison of the different experiments, the developed system can satisfy the required specification in Table 2 for the new generation of glass substrates.

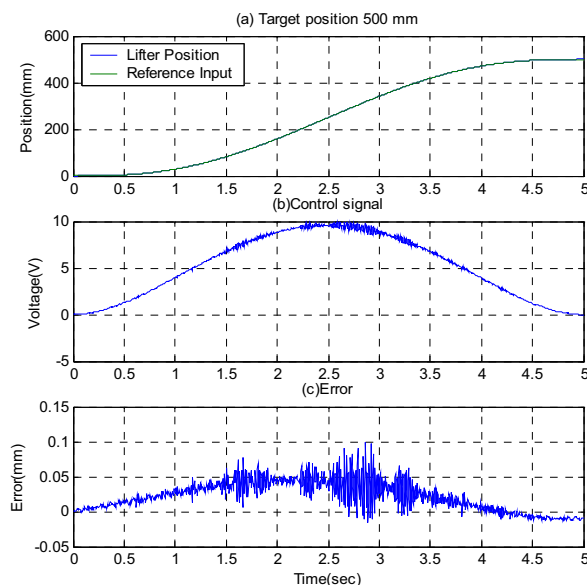


Figure 6 Experimental results of path-positioning control of lifting system

Table 4 Positioning control performance comparison

Path-positioning control			
Stroke (mm)	duration (sec)	Max.tracking error(mm)	End point error(mm)
100	10	0.026	-0.005
300	10	0.101	-0.003
500	10	0.101	-0.006
700	10	0.201	-0.007
100	5	0.026	0.006
300	5	0.065	0.006
500	5	0.099	-0.008

CONCLUSIONS

This paper proposed a novel pneumatic-balanced lifting positioning system for the new generation of flat panel display glass substrates. Through different experiments the feasibility and the repeatability can be confirmed. By means of the pneumatic-balanced control, the lifting positioning system driven by an AC servo motor can almost neglect the wide variation of the loading and achieve high position performance.

REFERENCES

1. TFT LCD Process Equipment Report, Display Search, 2006, U.S.
2. Flat Panel Display 2006, NIKKEI, 2006, Japan.
3. Neumann, R., Göttert, M., Konzepte zur Bahnregelung Servopneumatischer Antriebe, 5. Deutsch-Polnisches Seminar Innovation und Fortschritt in der Fluidtechnik, 2003, Warschau.
4. Hwang, G. C. and Chang, S., A stability approach to fuzzy control design for nonlinear system. *Fuzzy Sets Syst.*, 1992, Vol.48, pp.279-287.
5. Kim, S. W. and Lee, J. J., Design of fuzzy controller with fuzzy sliding surface. *Fuzzy Sets Syst.*, 1995, Vol.71, pp.359-369.
6. Lee, C. C., Fuzzy logic in Control Systems: Fuzzy logic Controller – part I, II. *IEEE Trans. Man, and Cybern.*, 1990, Vol.20, pp.404-435.
7. Lee, H. and Tomizuka, M., Robust adaptive control using a universal approximator for SISO nonlinear systems. *IEEE Trans. Fuzzy Syst.*, 2001, Vol.8, pp.95-106.
8. Maeda, M. and Murakami, S. A self-tuning fuzzy controller. *Fuzzy Sets Syst.*, 1992, Vol.47, pp.13-21.